

CDK2/cyclinA inhibitors: Targeting the cyclinA recruitment site with small molecules derived from peptide leads

Georgette Castanedo,^a Kevin Clark,^a Shumei Wang,^a Vickie Tsui,^a Mengling Wong,^a John Nicholas,^a Dineli Wickramasinghe,^b James C. Marsters, Jr.^a and Daniel Sutherlin^{a,*}

^aDepartment of Medicinal Chemistry, Genentech Inc., 1 DNA Way, South San Francisco, CA 94080, USA

^bDepartment of Molecular Oncology, Genentech Inc., 1 DNA Way, South San Francisco, CA 94080, USA

Received 11 October 2005; revised 23 November 2005; accepted 1 December 2005

Available online 27 December 2005

Abstract—The syntheses of potent small molecule inhibitors of the CDK2/cyclinA recruitment site are described. Structure–activity trends of nanomolar octapeptides were examined through amino-acid substitution and truncation of the sequence resulting in the identification of a smaller, albeit significantly less potent, tetrapeptide lead. These losses in affinity were recovered by side-chain optimization and by rigidification of the peptide backbone using a combination of solid-phase parallel synthesis and structure-based design. Finally, two guanidine functionalities were replaced to improve drug-like properties, resulting in neutral small molecules equal in activity to that of the peptide lead.

© 2005 Elsevier Ltd. All rights reserved.

Cell-cycle progression requires the coordinated interaction and activation of cyclins and cyclin-dependent kinases (CDKs). During S-phase, cyclinA (CycA) binds to CDK2 and activates the kinase as well as recruits substrates and inhibitors to the complex through a hydrophobic groove that is approximately 50 Å away from the CDK2 active site.¹ Blockage of this CycA recruitment site would allow a more selective approach to CDK inhibition than the standard active-site antagonists. The transcription factor E2F is a substrate for the CDK2/CycA complex and is phosphorylated as a prelude to S-phase exit. Cellular response to CDK2/CycA inhibition is thought to be greater in tumor versus normal tissue since E2F is commonly deregulated in tumor cells and has been reported to result in cell death in combination with CDK2/CycA inactivation.² Therefore, selective inhibition of this phosphorylation event should block S-phase exit and sensitize cancer cells to apoptosis. We have tested the consequence of cyclinA inhibition and validated this approach by using cell penetrating peptides that block the recruitment site on cyclinA and selectively kill cancer cells in vitro and in vivo.³ A small molecule derived from these proof-of-concept peptides with improved drug-like properties could

act as a selective anti-cancer agent. The few reported studies of recruitment site inhibitors have primarily focused on the SAR of endogenous peptide substrates or inhibitors of cyclinA as a guide for future small molecule design.⁴ This communication describes the optimization of a peptide lead to a potent small molecule ($IC_{50} = 6$ nM).

Endogenous substrates and inhibitors of the CDK2/CycA recruitment site have the consensus sequence RXL and require a second C-terminal hydrophobic amino acid either directly after the leucine or separated by an additional residue (p27-RNLF, E2F1-RRLDL). Crystal structures of peptides derived from these sequences bound in this site illustrate a shallow protein–protein interface.⁵ Peptide **1** (PVKRRLFG, Table 1)⁶ was used as our starting point and was tested in a CDK2/CycA ELISA using the retinoblastoma protein (Rb) as a substrate ($IC_{50} = 12$ nM).⁷ A peptide library was prepared to evaluate the contribution of each amino acid side chain. Alanine scanning of peptide **1** showed the most significant loss in activity for leucine and phenylalanine, and arginine replacement (peptides **5**, **7**, and **8**) consistent with the consensus sequence. The remaining residues had little or no effect on binding.

Truncation of the peptide from the N-terminus to the consensus sequence caused a 120-fold reduction in potency (peptides **10–12**). Truncation of the C-terminal

Keywords: CDK2/cyclinA; Protein–protein interaction inhibitor; Guanidine replacement.

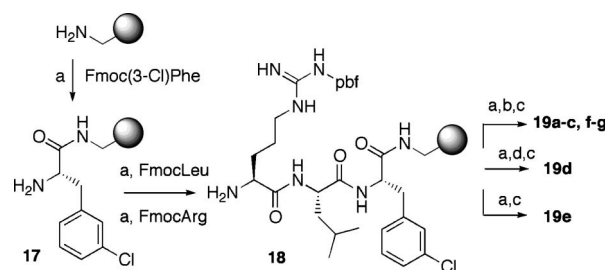
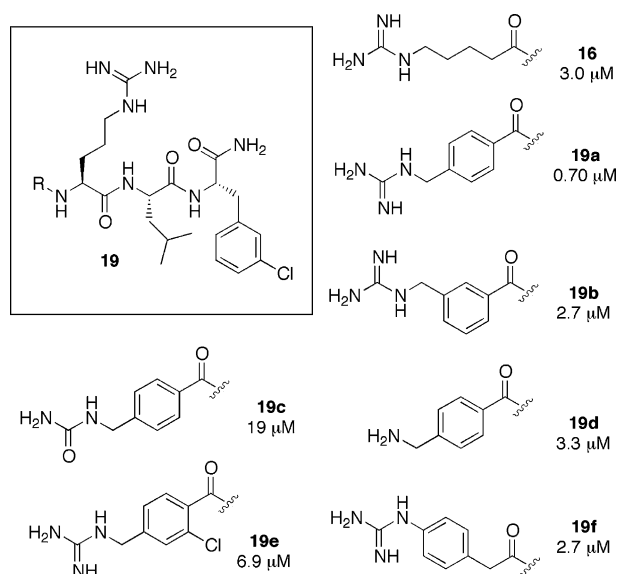
* Corresponding author. Tel.: +1 650 225 3171; fax: +1 650 225 2061; e-mail: dans@gene.com

Table 1. Peptide sequence length and side-chain contributions to binding

Compound	Sequence	IC ₅₀ (nM)	Fold diff.
1	PVKRRLLFG	12	—
2	AVKRRLLFG	16	1.3
3	PAKRRLLFG	10	0.8
4	PVARRLLFG	62	5.2
5	PVKARLLFG	1,600	130
6	PVKRALFG	130	11
7	PVKRRAFG	22,000	1800
8	PVKRRLAG	8200	680
9	PVKRRLFA	10	0.8
10	VKRRLLFG	120	10
11	KRRLLFG	770	64
12	RRLFG	1,400	120
13	PVKRRLLF	14	1.2
14	PVKRRLLF-NH ₂	28	2.3
15	PVKRRLL-(3-Cl)F-NH ₂	0.6	0.05
16	(desNH ₂)-RRL-(3-Cl)F-NH ₂	3000	250

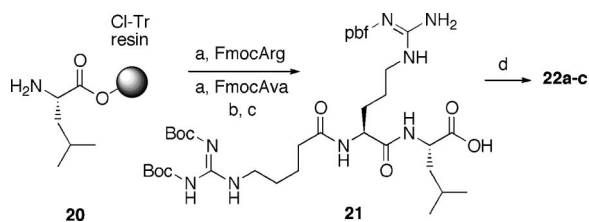
glycine, resulting in either the phenylalanine acid **13** or amide **14**, was well tolerated. Peptide libraries were prepared using a variety of templates with natural, unnatural, L, and D amino acids to probe the binding surface. Most analogs resulted in loss of activity to varying degrees, while substitution on the aryl ring of phenylalanine met with the greatest success. The substitution of phenylalanine with 3-chlorophenylalanine, illustrated in peptide **15**, resulted in a 10-fold improvement in potency relative to peptide **14**. These data are consistent with previously reported SAR with RXLIF peptides, where 4-halophenylalanines occupy a similar location in the binding pocket.^{5c} The lead peptide **16** resulted from a combination of C- and N-terminal truncations along with the 3-chlorophenyl alanine substitution and lacking the N-terminal amine (des-amino arginine for arginine). This 3 μ M peptide was significantly less potent than the lead peptide **1** but represented a more productive starting point for medicinal chemistry development due to its lower molecular weight and smaller size.

It was hypothesized that the binding energy of **16** could be increased through optimization of favorable interactions with the protein surface and the preorganization of the compound to the bound conformation. Resin-bound 3-chlorophenylalanine **17** was used in standard peptide synthesis techniques to prepare analogs **19a–g** (Scheme 1). The N-terminal flexible alkyl chain of the arginine mimetic **16** could be replaced with a more rigid aryl group to give compound **19a**. The 4-fold increase in activity upon incorporation of the *para*-guanidinomethylbenzoic acid (GMBA) in **19a** was consistently observed throughout several scaffolds (Fig. 1). Placing the guanidinomethyl substituent in the meta position, compound **19b**, was less effective but was equipotent with the straight chain compound **16**. The importance of the guanidine functionality in **19a** was illustrated by the urea **19c**, which was more than 27-fold less potent, and the benzyl amine **19d**, 5-fold less potent. No improvement in activity was obtained through ortho substitution of the aryl ring, designed to perturb the

**Scheme 1.** Reagents and conditions: To prepare compound **17**—Rink resin, (a) HOBt, HBTU, DIPEA, DMF, 4 h; then 20% pip/DMF, 10 min; (b) *N,N*-bis(*t*-butoxycarbonyl)-1*H*-pyrazole-1-carboxamide, DIPEA, DMF; (c) TFA; (d) TMSNCO, DIPEA. Pbf is 2,2,4,6,7-pentamethyldihydrobenzofuran-5-sulfonyl.**Figure 1.** Compounds **19**. N-terminal modifications and CDK2/CycA binding.

aryl-carbonyl rotational barrier (compound **19e**), or by changing the benzoic acid to a phenyl acetic acid (compound **19f**). When molecular models and, later, crystal structures developed from compounds similar to **19a** were examined, it became apparent that the guanidine group in the GMBA was not likely to contact cyclinA in the same location as the N-terminal guanidine of the full-length peptides. Rather, the *para*-substituted benzoic acid directs the guanidine to a separate region in the binding site that also has negative electrostatic potential, which was previously occupied by the backbone of the full-length peptides.

Having had some success in improving binding affinity by reducing conformational freedom, a similar approach was undertaken at the C-terminus. In order to prepare analogs, the protected intermediate **21** was prepared on chlorotrityl resin starting from resin-bound leucine **20** (Scheme 2). This advanced intermediate was then used in amide bond couplings with a variety of amines to prepare analogs **22**. The C-terminal amide in compound **16** could easily be replaced with hydrogen, illustrated by phenethylamine **22a** (Fig. 2). Replacement



Scheme 2. Reagents and conditions: to prepare compound **20** use 2-chlorotrityl resin, Fmoc-leucine, DIPEA, CH_2Cl_2 , 4 h; then 20% pip/DMF, 10 min; (a) HOBt, HBTU, DIPEA, NMP, 4 h; then 20% pip/DMF, 10 min; (b) *N,N*-bis(*t*-butoxycarbonyl)-1*H*-pyrazole-1-carboxamide, DIPEA, DMF; (c) 10% AcOH, 10% $\text{CF}_3\text{CH}_2\text{OH}$, CH_2Cl_2 , 2 h; (d) i. polystyrene-carbodiimide, polystyrene-HOBT, 10% DMF in CH_2Cl_2 , amine, 18 h; ii. TFA.

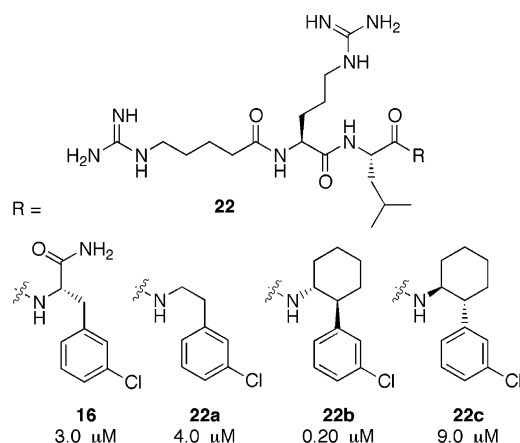


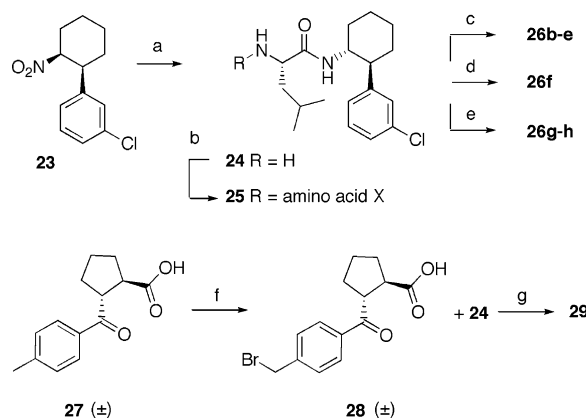
Figure 2. Compounds **22**. C-terminal modifications of the truncated peptide and CDK2/CycA binding.

of the chlorine in **22a** with either a fluorine or trifluoromethyl group was not effective, giving compounds with IC_{50} values of 18 and 42 μM , respectively (structures not shown). Potency was improved 20-fold by locking the chloro-phenyl group and the amide functionality into a gauche arrangement by replacing the phenethylamine with a *trans*-2-arylcylohexyl amine, giving compound **22b**. The dihedral angle between substituents of the 1,2-*trans*-disubstituted cyclohexane in **22b** is identical to the *N*- α -C β -Ph dihedral angle in reported structures of full-length RXLF peptides. The importance of the absolute stereochemistry is illustrated by diastereomer **22c**, which was more than 45-fold less potent. In order to further improve potency of compounds, combinations of these C-terminal and N-terminal modifications were pursued while also exploring the SAR of the internal arginine residue.

Given the success seen with the 3-chlorophenylcyclohexyl amine, all newly synthesized compounds were prepared using this functionality. Compounds (**26a–i**, Table 2) were prepared by base equilibration of 1-chloro-3-((1*S*,2*S*)-2-nitrocyclohexyl)benzene **23**⁸ (Scheme 3) to the *trans* stereochemistry followed by reduction of the nitro group using zinc and acetic acid (conditions used to preserve the chloro-arene functionality). The resultant amine was coupled to Boc-leucine and then deprotected

Table 2. Structure–activity relationships for compounds **26**

Compound	R	X	IC_{50} (nM)
26a	Guanidine	Arg	47
26b	Guanidine	Nle	31
26c	Guanidine	Ala	58
26d	Guanidine	dAla	31,000
26e	Guanidine	Pro	3,000
26f		Ala	251
26g		Ala	790
26h		Ala	21
26i		Abu	6.0



Scheme 3. Reagents and conditions: (a) i. NaHCO_3 , EtOH, 4 h, 99%; ii. Zn dust, AcOH, MeOH, 100%; iii. EDC, Boc-leucine, CH_2Cl_2 ; iv. HCl; (b) i. EDC, Boc amino acid X, CH_2Cl_2 ; ii. HCl; (c) i. EDC, Boc-4-(aminomethyl)benzoic acid; ii. HCl; iii. *N,N*-bis(*t*-butoxycarbonyl)-1*H*-pyrazole-1-carboxamide, DIPEA, DMF; (d) i. EDC, [4-(*N*-Boc-piperidiny)methyl]-4-benzoic acid, CH_2Cl_2 ; ii. HCl; (e) i. EDC, α -bromo-*para*-toluic acid, CH_2Cl_2 ; ii. 1-methyl-3-aminopyrazole or 2-aminothiazole, DMSO, 5 min, 130 °C; (f) NBS, benzoyl peroxide, 5% AcOH in benzene, 130 °C, 5 min, 54%; (g) i. EDC, CH_2Cl_2 ; ii. 2-aminothiazole, DMSO, 5 min, 130 °C.

to give dipeptide **24**. This intermediate was further elaborated with one variable amino acid (indicated as X in Scheme 3 and Table 2) to give compounds **25**. From this point the synthetic routes diverged in to access compounds containing guanidines **26a–e** or other functionalities **26f–i**.

When the constrained 3-chlorophenylcyclohexyl amine was used along with the N-terminal GMBA, a 5-fold improvement in binding was observed versus **22b** to give 47 nM compound **26a** (Table 2). The internal amino

acid “X” mainly served a structural purpose, illustrated by the substitution of the arginine in equipotent compound **26a** to nor-leucine **26b** or even the compact alanine **26c**. This observation was in contrast to the 10-fold loss in affinity observed when the arginine to alanine substitution was effected in the full-length peptide. The importance of the stereochemistry at this residue is demonstrated by compound **26d**, where the natural L-alanine has been exchanged with a D-alanine, resulting in a >500-fold loss in affinity. Substitution with proline (compound **26e**) also resulted in a compound with poor affinity.

Having replaced the internal arginine with the neutral and smaller alanine, the remaining guanidine functionality at the N-terminus was targeted for replacement. Substitutions retaining the positive charge in the general vicinity of the guanidine were explored and led to piperidine **26f**. We also surveyed weakly basic heterocycles that could be protonated once in proximity to the anionic region on the protein surface. This strategy was especially successful when an aminothiazole was used in place of the guanidine, yielding a 21 nM analog **26h**. The activity of this compound was further improved 3-fold via an effective one-carbon homologation of the alanine to α -aminobutyric acid giving compound **26i**.

Compound **26i** represents a significant advance over the truncated lead peptide **16** in that it is 500-fold more potent, contains fewer rotatable bonds, and is neutral at physiological pH. Anticipating that the peptidic nature of the compound may affect metabolism and oral adsorption, we sought to remove amide bonds from the molecule. Examination of crystal structures indicated a key hydrogen bond between the N-terminal amide

carbonyl and the protein surface. We reasoned that a ketone would be an ideal substitution for this amide and searched for available starting materials that would position a carboxamide and an aryl ketone in the appropriate geometry. *trans*-2-(4-Methylbenzoyl)cyclopentane-1-carboxylic acid **27** (Scheme 3) was incorporated into the optimized scaffold to yield the 40 nM compound **29** (Scheme 3, Fig. 3). This inhibitor was very close in potency to the alanine derivative **26h**, in contrast to the inactive proline compound **26e**. A model of this compound superimposed onto a crystal structure of the peptide fragment RNLf (Fig. 3) shows the ketone oxygen in the appropriate geometry to accept a hydrogen bond from glutamine 254 in CycA.⁹ The synthesis of **29** (Scheme 3) was initiated by bromination of racemic acid **27** and then coupling the resultant bromo-acid **28** with peptide **24**. It was at this point that the amino-thiazole was installed and the diastereomers were separated by reversed-phase HPLC. The diastereomer of **29** was inactive in the kinase ELISA. The stereochemical assignment of these diastereomers was inferred from the biochemical activities and through a comparison of both compounds modeled into the active site.

Many of the compounds detailed in Table 2 demonstrate that it is possible to obtain lower molecular weight compounds with equivalent or better affinity for cyclinA than natural octapeptides, which have previously been shown to selectively kill tumor cells when combined with cell penetrating sequences. The rigidification and preorganization of the side chains as well as improving hydrophobic contacts in the binding site were responsible for the dramatic increases in potency when compared to the simple truncated peptide leads. Namely, the *meta*-chlorophenyl, cyclohexylamine, and the GMBA moieties accounted for significant improvements in activity.

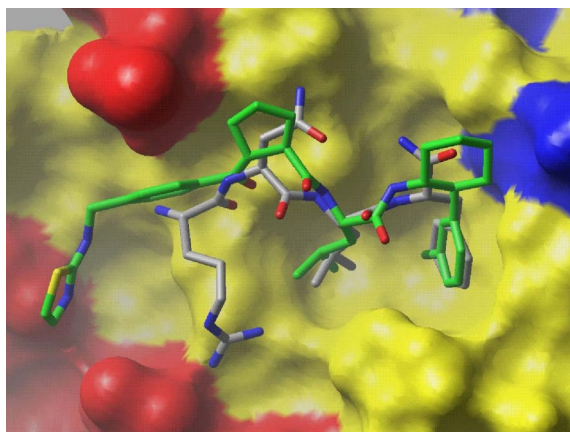
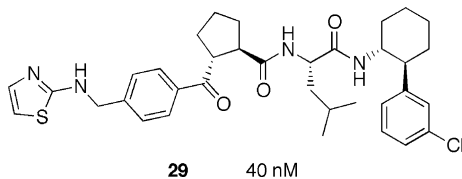


Figure 3. Molecular model of small molecule **29** in green bound to cyclinA and overlapped onto the crystal structure of a peptide containing the sequence RNLf in gray (PDB ID:1H27, Ref. 5b).

Acknowledgments

The authors thank Jenny Stamos for protein production and purification and Christian Wiesmann for crystallography.

References and notes

- Russo, A. A.; Jeffrey, P. D.; Patten, A. K.; Massague, J.; Pavletich, N. P. *Nature* **1996**, *382*, 325.
- Lees, J. A.; Weinberg, R. A. *Proc. Natl. Acad. Sci. U.S.A.* **1999**, *96*, 4221.
- (a) Chen, Y.-N. P.; Sharma, S. K.; Ramsey, T. M.; Jiang, L.; Martin, M. S.; Baker, K.; Adams, P. D.; Bair, K. W.; Kaelin, W. G. *Proc. Natl. Acad. Sci. U.S.A.* **1999**, *96*, 4325; (b) Mendoza, N.; Fong, S.; Marsters, J.; Koeppen, H.; Schwall, R.; Wickramasinghe, D. *Cancer Res.* **2003**, *63*, 1020.
- (a) Sharma, S. K.; Ramsey, T. M.; Chen, Y.-N. P.; Chen, W.; Martin, M. S.; Clune, K.; Sabio, M.; Blair, K. W. *Bioorg. Med. Chem. Lett.* **2001**, *11*, 2449; (b) Atkinson, G. A.; Cowan, A.; McInnes, C.; Zheleva, D. I.; Fisher, P. M.; Chan, W. C. *Bioorg. Med. Chem. Lett.* **2002**, *12*, 2501; (c) McInnes, C.; Andrews, M. J. I.; Zheleva, D. I.; Lane, D. P.;

- Fisher, P. M. *Curr. Med. Chem. Anti-Cancer Agents* **2003**, *3*, 57; (d) Zheleva, D. I.; McInnes, C.; Gavine, A.-L.; Zhelev, N. Z.; Fisher, P. M.; Lane, D. P. *J. Peptide Res.* **2002**, *60*, 257.
5. (a) Brown, N. R.; Noble, M. E. M.; Endicott, J. A.; Johnson, L. N. *Nat. Cell Biol.* **1999**, *1*, 438; (b) Lowe, E. D.; Tews, I.; Cheng, K. Y.; Brown, N. R.; Gul, S.; Noble, M. E. M.; Gamblin, S. J.; Johnson, L. N. *Biochemistry* **2002**, *41*, 15634; (c) Kontopidis, G.; Andrews, M. J. I.; Cowan, A.; Powers, H.; Innes, L.; Plater, A.; Griffiths, G.; Paterson, D.; Zheleva, D. I.; Lane, D. P.; Green, S.; Walkinshaw, M. D.; Fisher, P. M. *Structure* **2003**, *11*, 1537.
 6. (a) Adams, P. D.; Sellers, W. R.; Sharma, S. K.; Wu, A. D.; Nalin, C. M.; Kaelin, W. G. *Mol. Cell. Biol.* **1996**, *16*, 6623; (b) Takeda, D. Y.; Wohlschlegel, J. A.; Dutta, A. *J. Biol. Chem.* **2001**, *276*, 1993; (c) Wohlschlegel, J. A.; Dwyer, B. T.; Takeda, D. Y.; Dutta, A. *Mol. Cell. Biol.* **2001**, *21*, 4868.
 7. 96-well high-binding microtiter ELISA plates were coated overnight at 4 °C with mouse anti-GST in PBS. The plates were decanted and blocked with ELISA buffer (0.05% bovine γ -globulins [BGG] in 50 mM Tris-buffered saline [pH 7.5] with 0.05% Tween 20 and 0.1 mM sodium orthovanadate). The kinase reaction was performed in 96-well non-binding microtiter plates. ATP, CDK2/CycA (HIS tagged and phospho T160), and GST-Rb were diluted in kinase reaction buffer (25 mM Tris-buffered saline [pH 7.5] with 10 mM MgCl₂, 5 mM β -glycerophosphate, 2 mM DTT, 0.1 mM sodium orthovanadate, and 0.005% Nonidet P-40). Final concentrations of ATP and CDK2 were 200 μ M and 300 pM, respectively. Compounds were diluted in 10% DMSO in kinase reaction buffer. ATP was added to each well of the kinase reaction plate, followed in sequence by GST-Rb and test compound serial dilutions. The kinase reaction was started with the addition of CDK2/CycA to the kinase reaction plate and stopped with kinase stop buffer (50 mM EDTA in ELISA buffer). The ELISA plates were washed with ELISA wash buffer (50 mM Tris-buffered saline [pH 7.5] with 0.05% Tween 20 and 1 mM MnCl₂). The reactions were diluted 1:10 into kinase stop buffer in the ELISA plate. Phosphorylated Rb was detected with rabbit anti-phospho-Rb (Ser795) followed by (HRP)-linked IgG anti-rabbit antibody. The plate was developed with tetramethylbenzidine as substrate and the absorbance was measured at 450 nm.
 8. Hayashi, T.; Senda, T.; Ogasawara, M. *J. Am. Chem. Soc.* **2000**, *122*, 10716.
 9. The model was built from co-crystal structures of other peptides and peptidomimetics, and minimized in the CyclinA binding site using Schrodinger's MacroModel program.